Published in "Review of Scientific Instruments 89 (2): 025114, 2018"
which should be cited to refer to this work.

An arbitrary-function light power controller

Z. D. Grujić,[a] J. Piller, and A. Weis
Physics Department, University of Fribourg, CH-1700 Fribourg, Switzerland

We describe the design, applications, and performance of a simple light power controller. The device is built on a fiber-coupled electro-optic modulator with an active electronic feedback. It can be used to actively stabilize laser power or to impress an arbitrary waveform onto the power. The bandwidth of the device is ~70 kHz.

I. INTRODUCTION

Fiber-coupled electro-optical modulators (EOMs)[1] are widely used devices allowing the control of light power by a voltage. While in most (binary) optical telecommunication applications the light power has to be switched only between "high" and "low" values, many other scientific/technological applications call for a precise analog control of the light power with a linear voltage-to-power relation. In the latter case, the user has to take the EOM's highly nonlinear transfer function into account and further has to ensure stable environmental conditions, such as a constant EOM temperature.

Based on these requirements, we have designed a simple feedback-based arbitrary-function light power controller (AFPC) for our everyday laboratory experiments. Previously published approaches for compensating bias drifts have used active bias voltage stabilization based on bias modulation[2,3] and/or temperature stabilization.[2] The state-of-the-art photonic arbitrary waveform generator described in Ref. 4 uses three serially connected Mach-Zehnder modulators, driven by six digital 12.5 Gb/s signals.

In the AFPC described in Sec. II, the EOM temperature is passively stabilized by thermal contact to a massive load (optical table) and the output light power is made to synchronously follow a control set voltage using a proportional-integral (PI) controller.

II. PRINCIPLE OF OPERATION

The use of PI or proportional integral differential (PID) regulators is common practice in many process control applications.[5] The principle of our PI feedback-based light power controller is illustrated in Fig. 1. The output light power P_{out} is controlled by an input voltage, V_{set}, applied to a fiber-based EOM. A small fraction (2%) of the output light is detected by a monitor photodiode (PD), producing, after low-noise transimpedance amplification (TIA), a voltage V_{mon} that is proportional to the output light power. The sum of V_{set} and $V_{\text{mon}} \propto (-)P_{\text{mon}}$ forms the error signal that is amplified by parallel branches of a proportional amplifier (P) and an integrator (I), whose summed output voltages control the EOM. With a constant voltage V_{set} and properly adjusted PI parameters,[5] this feedback loop will ensure that P_{out} becomes independent of laser output fluctuations or drifts. Since $P_{\text{out}} \propto V_{\text{set}}$, any time-dependent set voltage $V_{\text{set}}(t)$ will force $P_{\text{out}}(t)$ to follow the set voltage on a time scale down to the inverse of the feedback loop's bandwidth.

A. Electro-optic modulator properties

The EOM's transfer function can slowly change over time due to (ambient or laser power related) temperature changes or wavelength/polarization[6,7] changes. The fiber-integrated EOM used in this work is the model AM905 from Jenoptik[8] that operates in a Mach-Zehnder interferometer configuration, optimized for the wavelength (894 nm) of the cesium D_1 transition. The interferometer is realized by splitting the input waveguide (polarization-maintaining, PM, fiber) into two parallel waveguides that have selected regions doped by x-cut $LiNbO_3$ and which are exposed to electric fields produced by oppositely poled electrodes. The coherent superposition interference of the modes propagating in the two arms, i.e., their constructive/destructive interference, will yield—after recombination—power, whose magnitude is determined by the differential phase shift, itself proportional to the voltage applied to the EOM, hence the voltage-controlled power control. This configuration greatly reduces the EOM's sensitivity to temperature drifts. The light transmission of the EOM is well represented by

$$T(V_{\text{m}}) = \frac{T_0}{2}\left[1 + \eta \sin\left(\pi \frac{V_{\text{m}} - V_{\text{bias}}}{V_\pi} - \varphi_0\right)\right], \qquad (1)$$

where V_{m} is the voltage applied to the modulation input and V_{bias} is the voltage applied to the bias input. ηT_0 is the maximal peak-peak modulation amplitude, where

$$\eta = \frac{T_{\max} - T_{\min}}{T_{\max} + T_{\min}} \qquad (2)$$

is the extinction ratio. $\varphi_0 = \pi V_0/V_\pi$ is an offset phase that the interferometer may have due to production imperfections, temperature gradients, and/or temperature changes. V_π is the so-called half-wave voltage, i.e., the voltage swing that switches the EOM from fully open to fully closed (Fig. 2). The bias voltage is adjusted to $V_{\text{bias}} = -V_0$ so that it compensates the offset phase.

[a]Electronic mail: zoran.grujic@unifr.ch

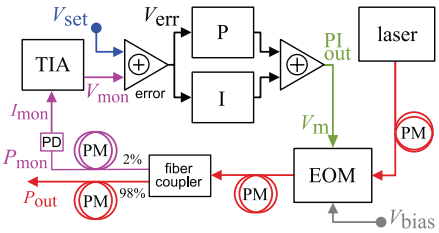

FIG. 1. Block scheme of the AFPC. Details are given in the text. Note that $V_{mon} = -R_T I_{mon}$, hence the addition in error signal generator.

The use of fiber-integrated small-sized x-cut $LiNbO_3$ crystals reduces the half-wave voltage (on the order of ~1 kV in free space crystals) to the very convenient range of ≈2-3 V, thus simplifying driver requirements and offering the potential of increasing the device's bandwidth to the many GHz range.

B. Realization of the electronic feedback circuit

A schematic diagram of the electronic circuit built for the active light power control is shown in Fig. 3. The monitoring light detector is a Thorlabs (model DET110) photodiode, in which a reverse bias voltage of 12 V from a battery reduces the internal capacitance, thus increasing the detector bandwidth. A transimpedance amplifier (TIA) with adjustable gain is used to convert the photocurrent I_{mon} into a voltage $V_{mon} = -R_T I_{mon}$.

A 10 pF capacitor C_T connected in parallel to the variable gain resistor R_T of the TIA prevents self-oscillation and limits the bandwidth of the amplifier to $f_{TIA}=(2\pi R_T C_T)^{-1}$ =32 kHz for C_T = 10 pF and R_T = 500 kΩ. The amplifier output is connected to a BNC connector for monitoring purposes and to a buffer amplifier before being transmitted to the error generator.

The error signal is obtained as the sum of V_{set} and the TIA signal $V_{mon} \propto -P_{mon}$. The proportional control is realized as an inverting amplifier with a variable negative feedback

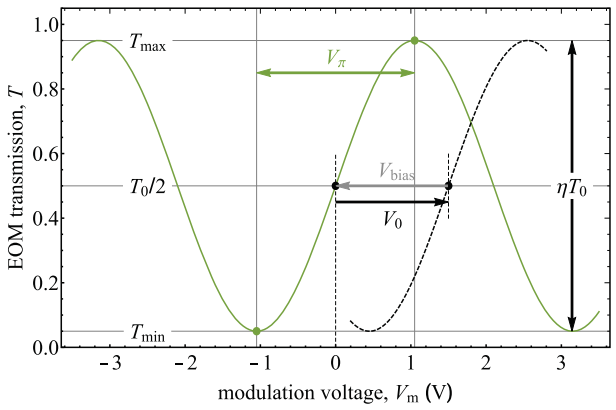

FIG. 2. The dotted (black) line shows part of the EOM's transfer function (for η = 0.9) that is dephased because of the (temperature dependent) intrinsic phase shift $\varphi_0 = \pi V_0/V_\pi$ of the device. The half-wave voltage is denoted by V_π. The solid (green) line shows the same transfer function when a bias voltage $V_{bias} = -V_0$ that compensates φ_0 is applied.

resistor R_{P2} for gain control. The time constant $\tau_I = R_I C_I$ of the PI's integrator is defined by a variable input resistor R_I and a tantalum capacitor C_I. The PI signal is obtained as a weighted sum of the signals from the proportional and integrator paths, with relative weights determined by R_{PW} and R_{IW} (variable).

A final buffer amplifier is used to produce a current that can drive the EOM's input's resistance of 50 Ω. The 400 Ω resistor connected in series with the EOM limits the peak-to-peak PI controller output to a voltage of $\approx V_\pi$ which, in combination with a suitable bias voltage $V_{bias} = -V_0$ [Eq. (1)], limits the EOM's working range to the positive slope region (labeled by V_π) in Fig. 2.

The transfer function of the PI controller is given by

$$f(t) = g_P V_{err}(t) + g_I \int_0^t V_{err}(t')dt', \qquad (3)$$

where the parameters defining the proportional gain $g_P = -R_{P2}/R_{P1}$ and integrator time constant $g_I = -(R_I C_I)^{-1}$ are independently adjustable by corresponding potentiometers. Instructions on how to optimize g_P and g_I are given, e.g., in Ref. 5.

III. DEVICE PERFORMANCE FOR LARGE AND SMALL AMPLITUDE MODULATION

A. Bandwidth of the AFPC

We have measured the AFPC bandwidth in the following way: A sine-wave oscillating at frequency f was applied to the V_{set} input of the electronics (Fig. 1), and the amplitude V_{exp} of the resulting light power modulation at the location marked P_{out} in Fig. 1 was measured by lock-in demodulation of a photodiode signal at that location. Plotting $G(f) = V_{exp}(f)/V_{exp}(f \ll f_{-3\,dB})$ as a function of f yields the transfer function shown in Fig. 4. The data points (black dots) are well fitted by a low-pass filter function, yielding a −3 dB bandwidth of ~71 kHz. The speed of the detected signal was limited by the used amplifier's (Femto,[9] model DLPCA-200) bandwidth f_F of 500 kHz. Data points above that frequency (vertical dashed red line in Fig. 4) were therefore excluded from the fit.

B. Pulse response of the AFPC

Another important test for understanding device performance is its pulse response. Figure 5 shows the response of the AFPC to square pulses of different amplitudes. The recorded light power responses are distorted because of AFPC-specific bandwidth limitations. Based on the data of Fig. 4, one expects exponentially rising and falling edges with a time constant τ of $1/(2\pi f_{-3\,dB}) \cong 2.24$ μs in the time domain. This behavior is well reproduced by the actual measurement of a small (≈10% of full range) amplitude pulse shown in Fig. 6. For modulation amplitudes comparable with the full range, the system response will slow down significantly because of the EOM's nonlinear transfer function [Eq. (1)].

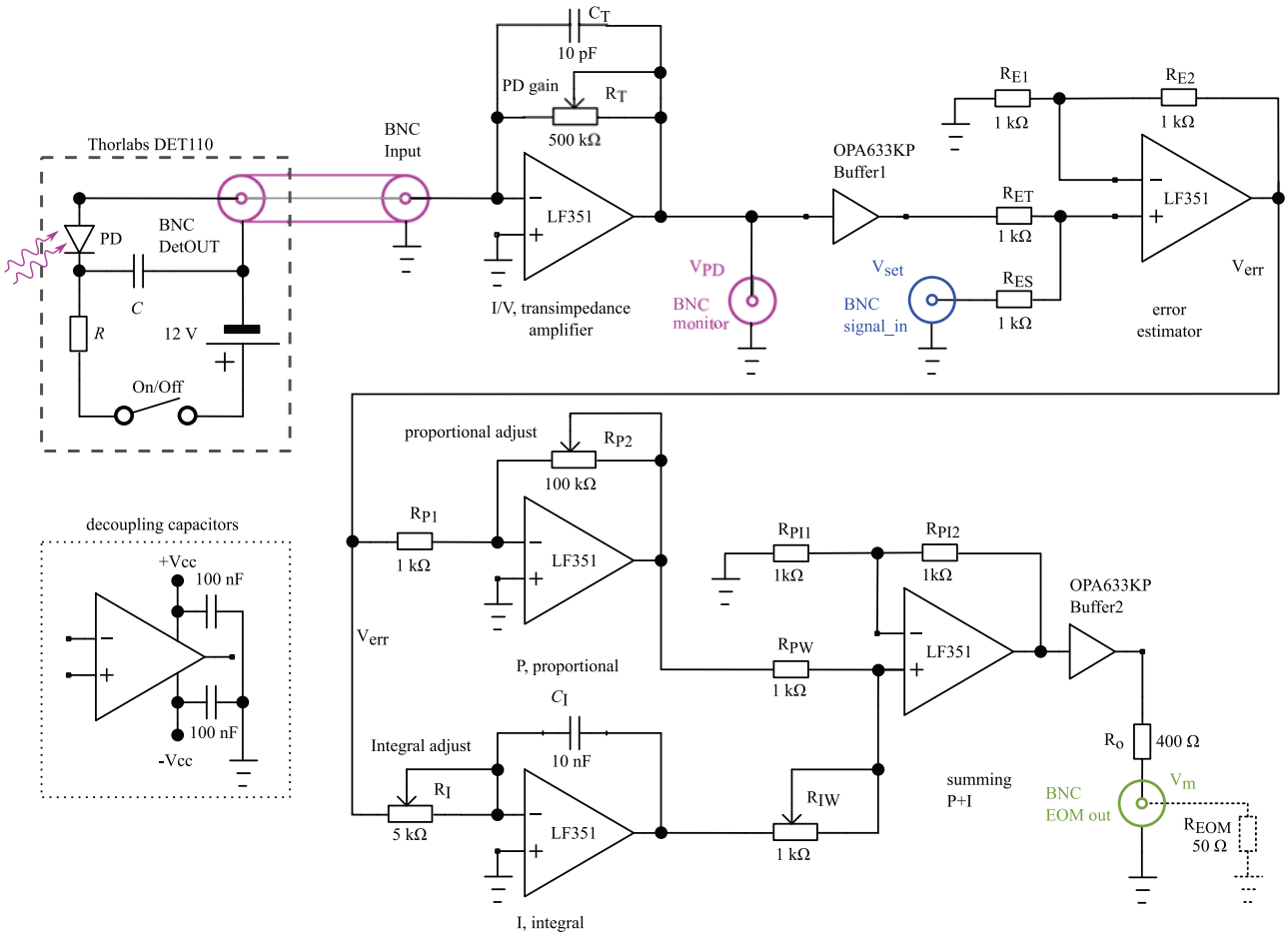

FIG. 3. Electronic block scheme of the transimpedance amplifier followed by a PI controller that is at the heart of the AFPC. The 100 nF decoupling capacitors (see the inset on the lower left) protect the power inputs of all operational amplifiers. All colors refer to the color coding in Fig. 1.

IV. APPLICATIONS

The AFPC is a device that allows stabilizing the power of a laser beam (using $V_{\rm set}$ = const) or, alternatively, forcing the laser power to follow a given time-dependence imposed by $V_{\rm set}(t)$. In Secs. IV A–IV D, we list a few applications for which the AFPC has proven to be a useful device.

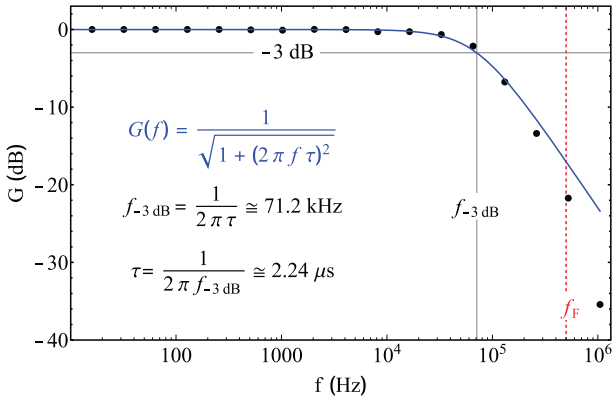

FIG. 4. The black points represent the measured AFPC frequency response, and the blue line is a fit by a first order low-pass filter function. The dashed (red) vertical line at $f_{\rm F}$ = 500 kHz marks the bandwidth of the transimpedance amplifier (Femto,[9] model DLPCA-200) used to measure the power modulation amplitude at the experiment's location.

A. Nonlinear spectroscopy

In a typical nonlinear optics experiment, one measures a certain physical property Q as a function of the power P of incident light. Such a measurement is often done by attenuating the incident light power by (discrete or variable) neutral density filters or by a combination of wave-plates and polarizers. Such a procedure implies a separate measurement of the power for each step of attenuation. Use of the AFPC is a more

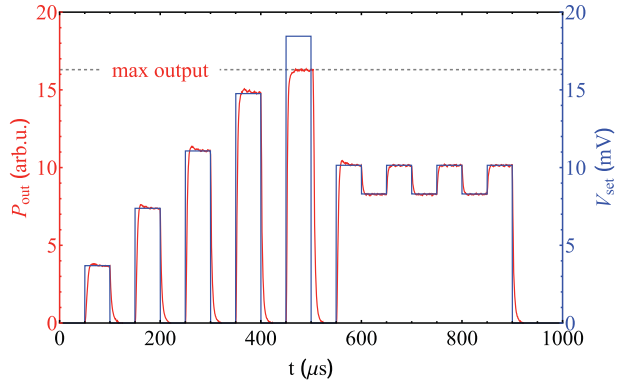

FIG. 5. Square pulse response. The AFPC has different response times depending on the local slope of the EOM's transfer function. Here we demonstrate the system reaction to square pulses of different amplitudes.

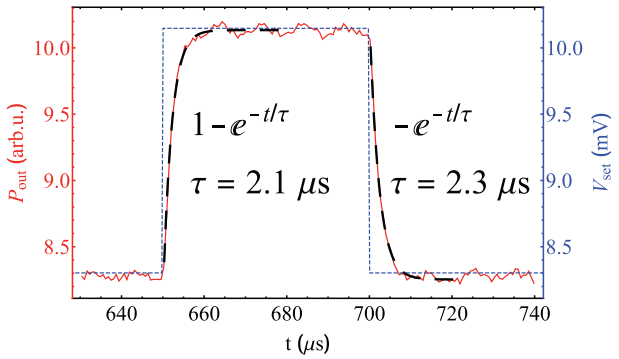

FIG. 6. Zoom into a selected pulse from Fig. 5. The black dashed lines represent exponential fits to the rising and falling edges.

time-efficient means for achieving the same goal: Driving the V_{set} input by a linear ramp that also drives the x-axis of an x–y oscilloscope and connecting the signal representing the physical property Q to the y-input allow a direct visualization of the $Q(V_{set})$ dependence, which after calibration yields the $Q(P)$ dependence of interest. The time axis needs of course to be calibrated, which is achieved by once inserting a power meter in front of the actual experiment and recording the $P(V_{set})$ dependence.

B. Hyperfine spectrum of the Cs D_1 line

In many spectroscopic experiments, it is advantageous to have a light power that does not vary with the laser frequency. Figure 7 shows a spectrum $P_t(\omega)$ of the 4 hyperfine components of the Cs D_1 transition. The spectrum is obtained by scanning the frequency ω_L of a single-mode extended cavity diode laser (ECDL) and recording the power P_t transmitted by a cell containing a vapor of Cs atoms. ECLDs have the property that their output power grows with increasing wavelength, i.e., with decreasing frequency. As a consequence, the absorption lines are superposed on a background that varies across the spectrum [Fig. 7(a)]. In general, this background can be well fitted by a polynomial function of suitable order. The presence of background affects the accuracy with which the spectroscopic quantities of interest (line amplitudes, widths, center frequencies) can be extracted. The bottom curve [Fig. 7(b)] illustrates the flattening of the background when the same spectrum is recorded using the AFPC with a fixed V_{set} voltage.

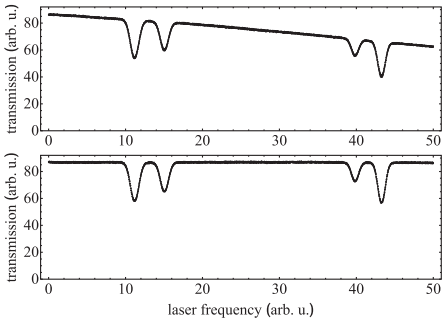

FIG. 7. Transmission spectrum of the cesium D_1 line without (top) and with (bottom) laser power stabilization by the AFPC.

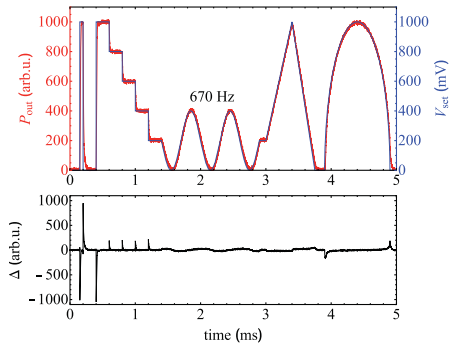

FIG. 8. Example of imprinting an arbitrary time-dependent voltage V_{set} (blue line) onto the laser power P_{out}. The trace Δ in the lower graph represents the difference between desired and obtained outputs, which is inevitably large for full ($\approx V_\pi$) swing modulation.

C. Free spin precession

In a recent article,[10] we have reported on the creation of spin-orientation in Cs vapor contained in a paraffin-coated cell by amplitude- (i.e., power-) modulated circularly polarized light. Following the polarization process, the freely precessing spin polarization was read out by the same laser beam with a power adjusted to a constant, small power. The AFPC has proven to be an extremely valuable tool for studying and optimizing the parameters (duty cycle, amplitude, frequency and duration) of the square-wave amplitude modulation in that experiment. In fact, we have developed the power controller specifically for that purpose but have identified several other applications in consequence. In particular, the ability of the AFPC to produce a very low power (limited only by the EOM's extinction ratio) on demand is crucial for many optimal optical pumping/probing experiments. Moreover, the fact that the high degree of repeatability of the device—even under conditions of a drifting V_0 phase—allows taking long term measurements that would be almost impossible otherwise.

D. Arbitrary waveform

The top graph of Fig. 8 shows an example of a controlled power variation following a generated arbitrary function consisting—in sequence—of a 50 μs long pulse, a staircase, two periods of a sine-wave, a linear ramp, and a parobolically shaped waveform, the complete waveform lasting 5 ms. The blue line represents the time trace $V_{set}(t)$ of the set voltage, while the overlaid red line represents the actually delivered time-varying laser power. The lower part of the figure represents the difference of the appropriately scaled detected power $P_{out}(t)$ (Fig. 1) and $V_{set}(t)$.

V. CONCLUSION

We have presented a simple electronic circuit which, together with a fiber-based EOM, allows imprinting arbitrary temporal light power changes onto a laser beam within a bandwidth of 71 kHz. This arbitrary-function light power controller (AFPC) is a versatile instrument for many applications in laser spectroscopy, nonlinear spectroscopy, and

magneto-optical experiments, to give just a few examples. In its current state, the AFPC's bandwidth is limited to ~70 kHz (Fig. 4) which, however, may be sufficient for many applications in laser spectroscopy labs. One advantage of the device is the relatively simple design of the electronics that—in our case—was assembled by an MSc student (JP) on a raster printed circuit board (PCB) mounted in the (Toptica,[11] model DC 110) rack of the laser driver.

The described AFPC was designed to meet our specific demands of a few 10 kHz bandwidth and perform well in this respect. The main bandwidth limitation comes from the LF351 operational amplifier's 100 kHz gain-bandwidth product, while the used photodiode (DET110 by Thorlabs) can go up to 15 MHz, and the EOM has a sub-ns rise time. Using suitable photodetection and electronic components, we believe that the described method could be extended to bandwidths of several 100 MHz. Moreover, the linearity of the system could profit from a non-linear gain amplifier that would compensate for the shape of the EOM's transfer function given by Eq. (1), a feature that goes beyond the goal of our project.

ACKNOWLEDGMENTS

The authors thank Emmanuel Gendre for skillful assistance with the electronics.

[1] E. L. Wooten, K. M. Kissa, A. Yi-Yan, E. J. Murphy, D. A. Lafaw, P. F. Hallemeier, D. Maack, D. V. Attanasio, D. J. Fritz, G. J. McBrien, and D. E. Bossi, IEEE J. Sel. Top. Quantum Electron. **6**, 69 (2000).

[2] D. T. Bui, C. T. Nguyen, I. Ledoux-Rak, J. Zyss, and B. Journet, Meas. Sci. Technol. **22**, 125105 (2011).

[3] J. Snoddy, Y. Li, F. Ravet, and X. Bao, Appl. Opt. **46**, 1482 (2007).

[4] P. K. Kondratko, A. Leven, Y.-K. Chen, J. Lin, U.-V. Koc, K.-Y. Tu, and J. Lee, IEEE Photonics Technol. Lett. **17**, 2727 (2005).

[5] U. Tietze and C. Schenk, *Halbleiter-Schaltungstechnik* (Springer, 2002).

[6] G. Li and P. Yu, J. Lightwave Technol. **21**, 2010 (2003).

[7] R. L. Jungerman, C. Johnsen, D. J. McQuate, K. Salomaa, M. P. Zurakowski, R. C. Bray, G. Conrad, D. Cropper, and P. Hernday, J. Lightwave Technol. **8**, 1363 (1990).

[8] See https://www.jenoptik.com for Jenoptik optical systems GmbH; accessed 05 May 2017.

[9] See http://www.femto.de/ for FEMTO® Messtechnik GmbH; accessed 15 May 2017.

[10] Z. D. Grujić, P. A. Koss, G. Bison, and A. Weis, Eur. Phys. J. D **69**, 135 (2015).

[11] See http://www.toptica.com/ for TOPTICA Photonics AG; accessed 10 October 2017.